CHAPTER IV

RESULTS AND DISCUSSION

(SYNTHESIS AND CHARACTERIZATION OF POLYBENZOXAZINE)

In the present study, the improvement of textural parameters has become the focus to increase the surface area of adsorbents derived from polybenzoxazine. As a result, the CO_2 adsorption capacity can be enhanced. The sol-gel technique was proposed to increase the surface area and porosity in polybenzoxazine.

In case of carbon aerogel preparation, phenol-based polybenzoxazines from two different types of amine precursors (i.e., diethylenetriamine (DETA) and pentaethylenehexamine (PEHA)) are synthesized by a sol-gel technique using xylene as a solvent, followed by carbonization in nitrogen and activation with CO_2. Moreover, the concentrations of benzoxazine monomer were varied at 30, 35 and 40 wt% in order to tune the surface properties of these porous polybenzoxazines. Furthermore, the influence of non-ionic surfactant (PEG-PPG-PEG block copolymer) loading on carbon aerogels was investigated.

4.1 Characterization of Materials

4.1.1 Characterization of Benzoxazine Monomer

Fourier Transform Infrared Spectrometer (FTIR) was employed to obtain an infrared spectrum of absorption band and evaluate the functional groups of the benzoxazine monomers synthesized from two different types of amine precursors, namely diethylenetriamine (DETA) as shown in Figure 4.1 and pentaethylenehexamine (PEHA) as shown in Figure 4.2. In the FTIR spectra of benzoxazine monomer, the peaks in the region of 920-950 cm^{-1} refer to the out of plane C-H vibration of the benzene attached to an oxazine ring as represented at the bands of 931 cm^{-1} from Figure 4.1 and 932 cm^{-1} from Figure 4.2. Whereas the adsorption bands at about 1230 and 1036 cm^{-1} were assigned to the asymmetric and symmetric stretching of C-O-C of oxazines which confirm the presence of the aromatic ether stretching as indicated at the bands of 1256 cm^{-1} from Figure 4.1 and 1257 cm^{-1} from Figure 4.2.

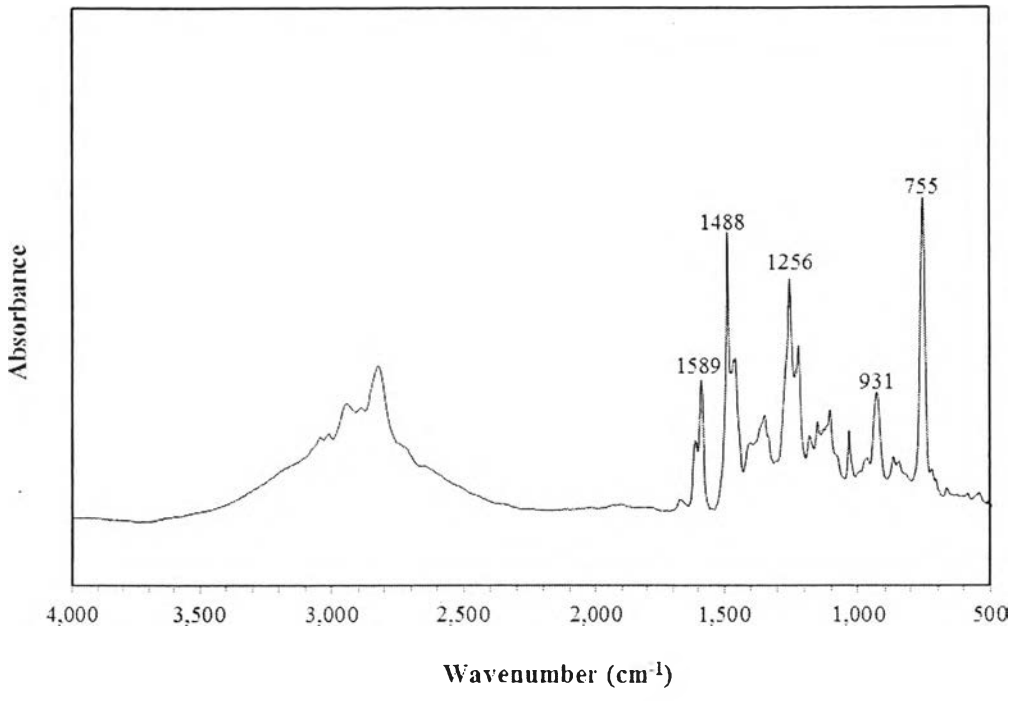

Figure 4.1 FT-IR spectrum of the benzoxazine monomer by DETA as reactant.

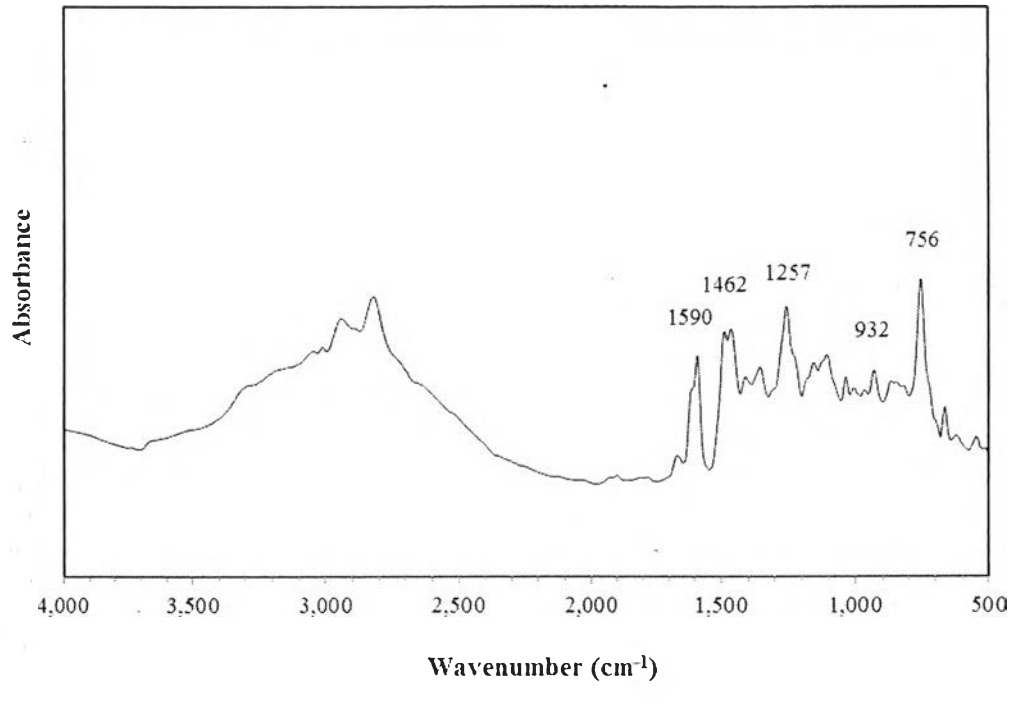

Figure 4.2 FT-IR spectrum of the benzoxazine monomer by PEHA as reactant.

The bands at 1488 cm^{-1} from Figure 4.1 and 1462 cm^{-1} from Figure 4.2 were assigned to the di-substituted benzene ring. Additionally, the out of plan bending vibrations of aromatic C-H at 713-821 cm^{-1} were detected for each benzoxazine monomer obtained as shown at 755 cm^{-1} from Figure 4.1 and 756 cm^{-1} from Figure 4.2. These FTIR results agree with the studies of Lorjai *et al.* (2009); Kiskan and Yagci (2014); Zhu *et al.* (2014).

The curing behavior of benzoxazine monomer was investigated by using a DSC with a heating rate of 10 °C/min under nitrogen atmosphere. Figure 4.3 illustrates the DSC thermograms of curing exothermic peak of benzoxazine monomers by DETA and PEHA as amine precursors. As seen from the figure, the exothermic peak of benzoxazine monomer synthesized from DETA, corresponding to its ring opening polymerization, was located between 120 and 190 °C, while the curing exothermic peak of benzoxazine monomer derived from PEHA as reactant was located from 130 to 200 °C. The heat of the reaction determined from the area under the exothermic peak was 16.56 and 42.83 J/g for DETA-derived benzoxazine monomer and PEHA-derived benzoxazine monomer, respectively.

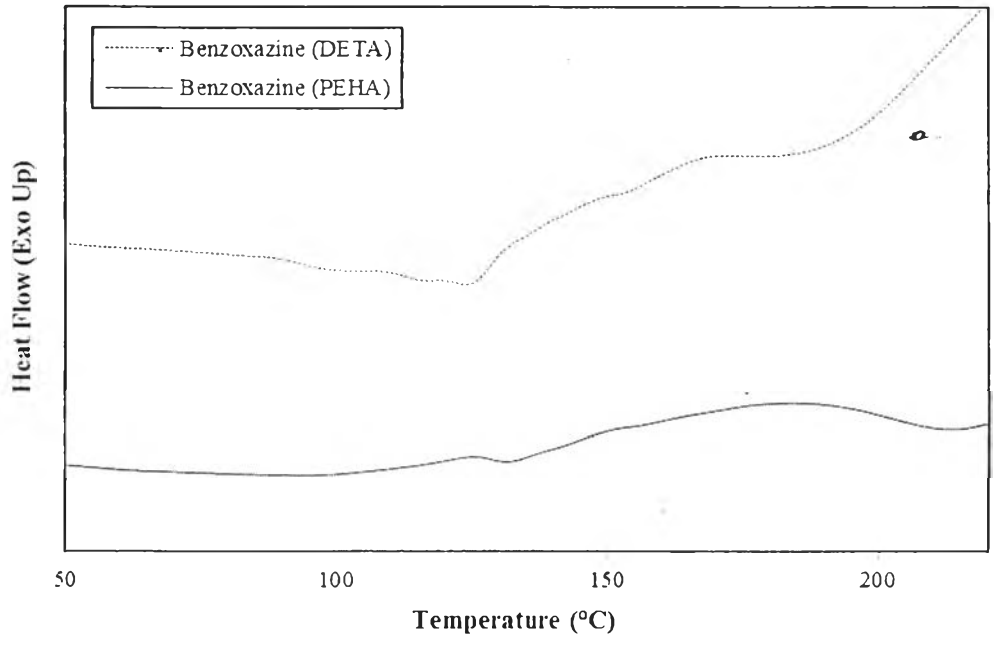

Figure 4.3 DSC thermograms of benzoxazine monomers by DETA and PEHA as reactants.

The decomposition temperature of both benzoxazine monomers was obtained by a TGA analyzer. The TGA thermograms of DETA-derived benzoxazine monomer and PEHA-derived benzoxazine were presented in Figure 4.4. Both benzoxazine monomers began to lose weight before 100 °C due to the remaining moisture in their structure and then stabilized at around 200 °C because of the transformation of benzoxazine monomer to polybenzoxazine during heating. The largest maximum mass loss rate of these benzoxazine monomers was occurred in the temperature ranges of 200 - 600 °C as a result of the production of a large amount of volatile materials. The rate of mass loss became slower after 600 °C and the mass loss could not be observed beyond 800 °C. Moreover, benzoxazine monomer derived from PEHA showed less amount of char yield (~15 wt%) than DETA-derived benzoxazine monomer (~30 wt%) because of the carbon-carbon bonds of long aliphatic chains were easily broken at high temperature, resulting in less char yield.

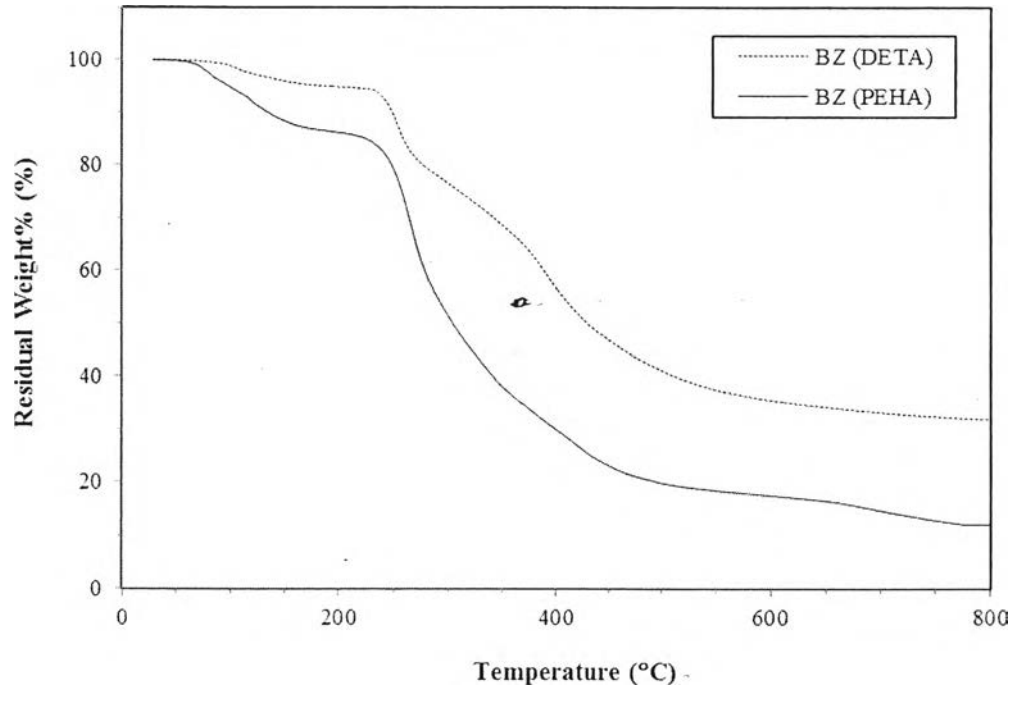

Figure 4.4 TGA thermograms of benzoxazine monomers with DETA and PEHA asamine reactants.

4.1.2 Characterization of Polybenzoxazine

The FT-IR spectra of polybenzoxazines synthesized from two different types of amine precursors, which are diethylenetriamine (DETA) as shown in Figure 4.5 and pentaethylenehexamine (PEHA) as shown in Figure 4.6, have been used to examine the ring opening polymerization of benzoxazine monomer. After a curing step at 120 °C for 30 min, 160 °C for 1 hr and 180 °C for 45 min, the characteristic absorption band at 920-950 cm^{-1} nearly disappeared due to the ring opening polymerization of benzoxazine monomer as shown at 932 cm^{-1} in Figure 4.5 and 934 cm^{-1} in Figure 4.6 for DETA-derived PBZ and PEHA-derived PBZ, respectively. The characteristic absorption bands of the polybenzoxazines between 1500 cm^{-1} and 1700 cm^{-1} in Figures 4.5 (DETA-derived PBZ) and 4.6 (PEHA-derived PBZ) demonstrated higher intensity than both benzoxazine monomers (see Figure 4.1 for DETA-derived BZ and Figure 4.2 for PEHA-derived BZ), showing the complete polymerization of the ring-opening mechanism. The intensity of adsorption bands at 1461 cm^{-1} from Figure 4.5 and 1459 cm^{-1} from Figure 4.6 has shifted from that of its monomer due to the increasing of tri-substituted benzene rings as agree with many other studies (Lorjai *et al.*, 2009; Zhang *et al.*, 2014; Zhu *et al.*, 2014).

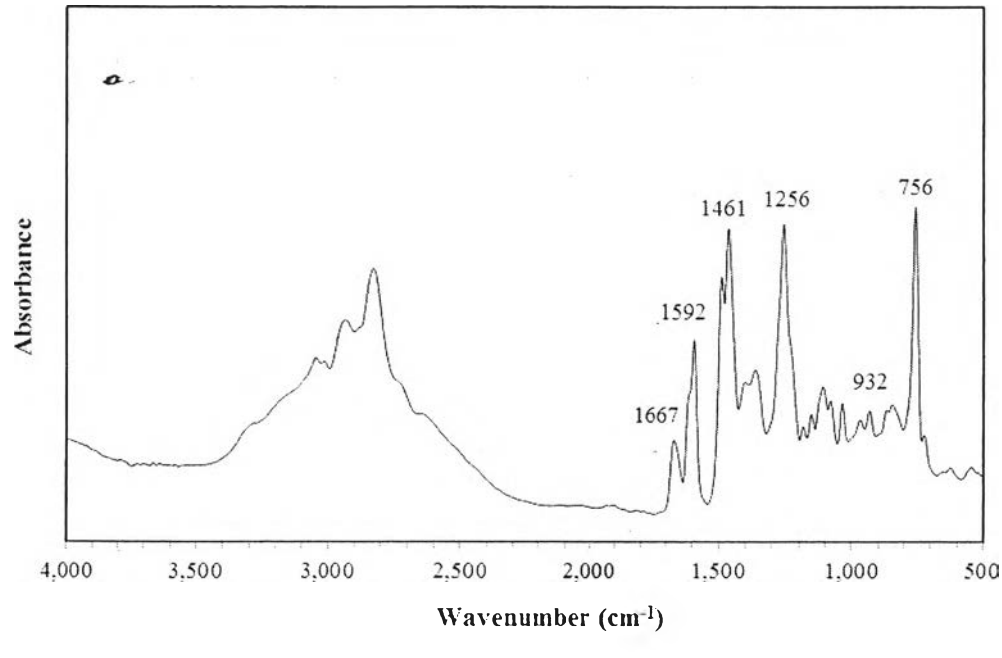

Figure 4.5 FT-IR spectrum of polybenzoxazine by DETA as reactant.

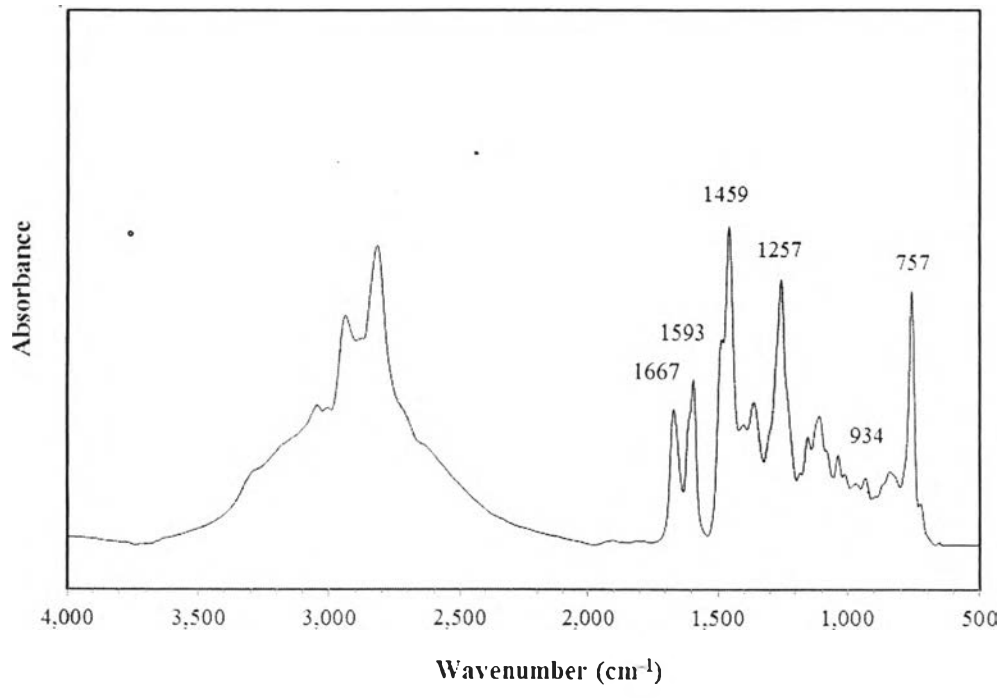

Figure 4.6 FT-IR spectrum of polybenzoxazine by PEHA as reactant.

The obvious progress of the ring opening polymerization from benzoxazine precursor was investigated by using a DSC analyzer with a heating rate of 10 °C/min from 30 to 180 °C under nitrogen atmosphere. After curing step at 120 °C for 30 min, 160 °C for 1 hr and 180 °C for 45 min, the exothermic peak totally disappeared, suggesting the completion of polymerization as shown in Figure 4.7 for DETA-derived polybenzoxazine and PEHA-derived polybenzoxazine.

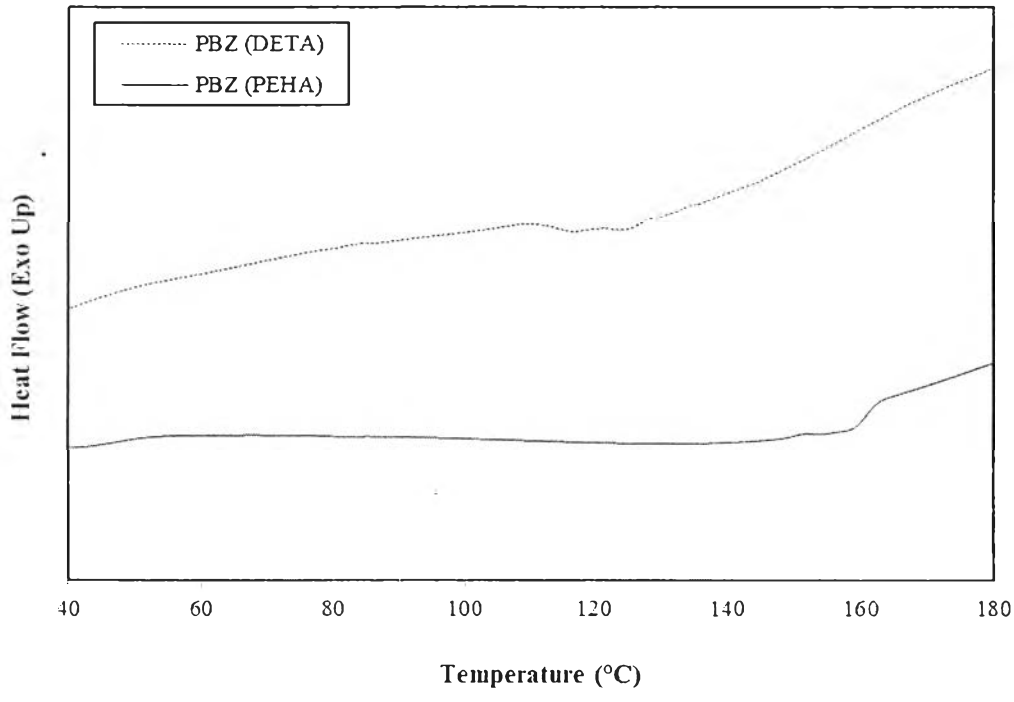

Figure 4.7 DSC thermograms of polybenzoxazines by DETA and PEHA as reactant.

Figure 4.8 illustrates the curing behaviors of the polybenzoxazine aerogels at the different curing time, DSC was used with a heating rate of 10 °C/min. After the curing step at 160 °C for 1 hr and 180 °C for 15 min, 30 min, and 45 min (Figures 4.8a, 4.8b, and 4.8c), the area of exothermic peak was reduced from 16.56 J/g of DETA-derived benzoxazine monomer to 7.97 and 3.70 J/g of the polybenzoxazine aerogels from a 40 wt% monomer solution at a curing time of 15 and 30 min, respectively. As clearly seen in this figure, the exothermic peak at around 160 - 200 °C of the DETA-derived aerogel from 40 wt% monomer solution at curing time of 45 min was completely disappeared. This evidence could imply that the curing reaction of polybenzoxazine was successful. Therefore, the curing condition of all organic aerogels was suggested at 160 °C for 1 hr and 180 °C for 45 min. On top of that, Figure 4.8c showed the glass transition temperature (T_g) which located between 150 and 170 °C related to polymer chain mobility and packing. This result agreed with the study of Kim and Ishida (2003).

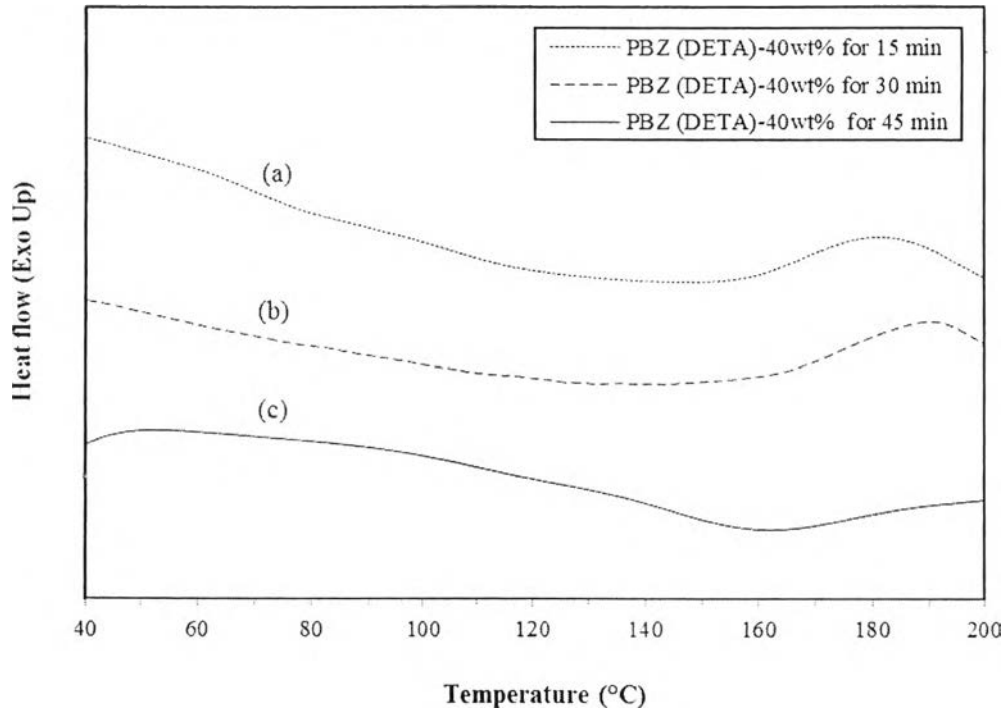

Figure 4.8 DSC thermograms of (a) DETA-40wt% derived aerogel at 180 °C for 15 min, (b) DETA-40wt% derived aerogel at 180 °C for 30 min, and (c) DETA-40wt% derived aerogel at 180 °C for 45 min.

After obtaining the curing condition of polybenzoxzine aerogels, different concentrations of aerogel were prepared at 30, 35, and 40 wt% using xylene as a solvent. Figures 4.9 and 4.10 illustrate the curing behaviors of DETA-derived polybenzoxazine aerogels with different benzoxazine concentrations. Before the curing step, the area of exothermic peak was 0.46, 2.97 and 18.84 J/g of polybenzoxazine aerogels from the solution with concentration of 30, 35 and 40 wt%, respectively. After the curing step, all exothermic peak of DETA-derived polybenzoxazine aerogels at around 160 - 200 °C disappeared, suggesting that the polymerization was complete.

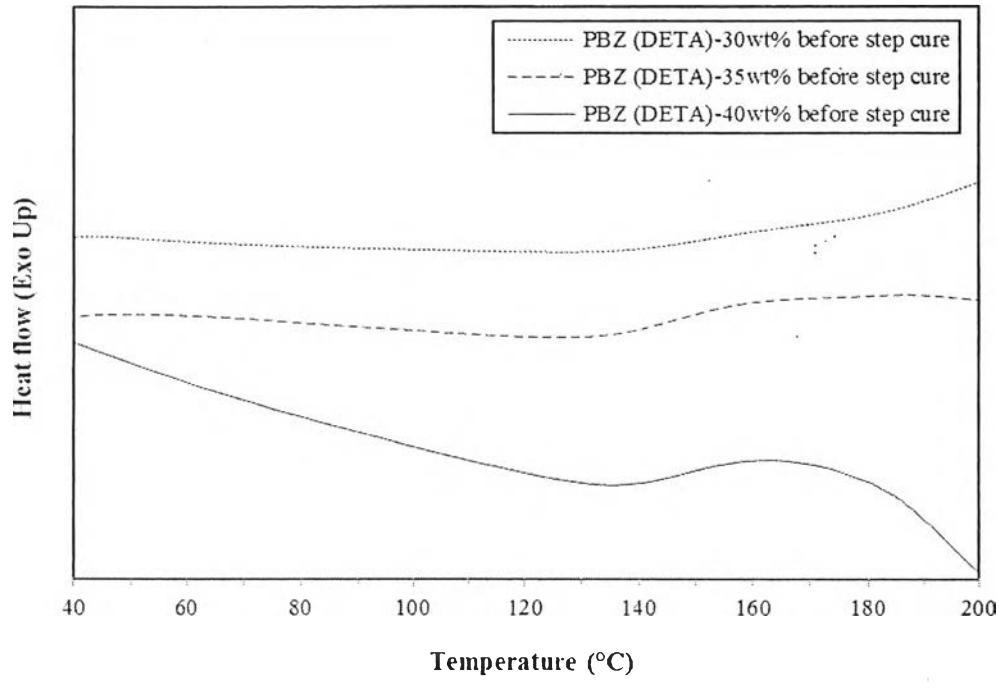

Figure 4.9 DSC thermograms of polybenzoxazine aerogels before curing step with DETA as reactant.

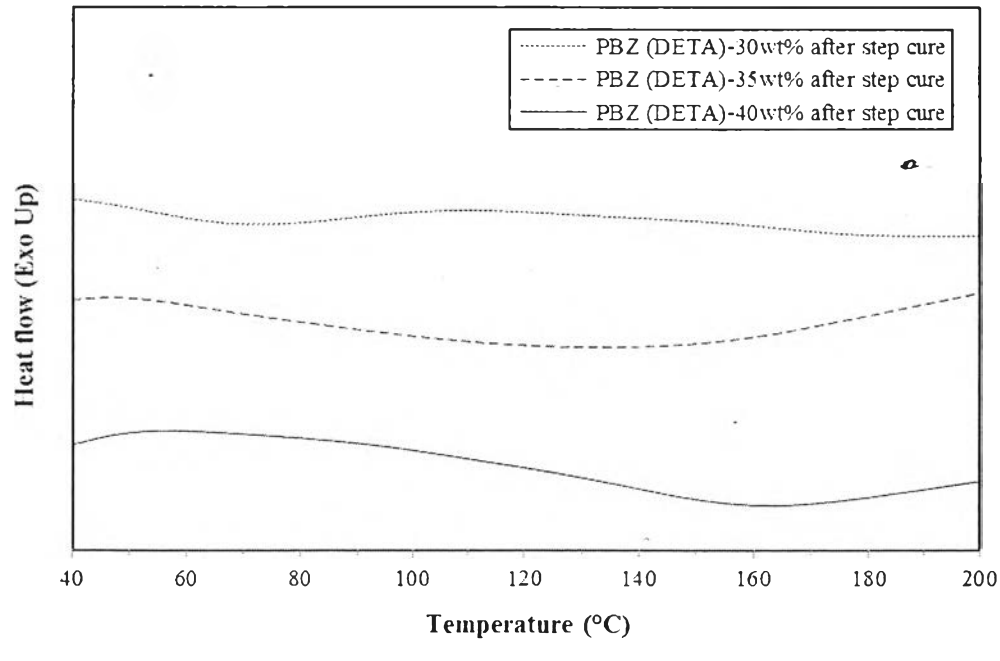

Figure 4.10 DSC thermograms of polybenzoxazine aerogels after curing step with DETA as reactant.

Figures 4.11 and 4.12 illustrate the curing behaviors of PEHA-derived polybenzoxazine aerogels with different benzoxazine concentrations. Before the curing step, the area of exothermic peak was at 4.69, 4.44 and 8.11 J/g of polybenzoxazine aerogels from the solution with concentration of 30, 35 and 40 wt%, respectively. After the curing step, all exothermic peak of PEHA-derived polybenzoxazine aerogels at around 160 - 200 °C disappeared, suggesting that the polymerization was complete.

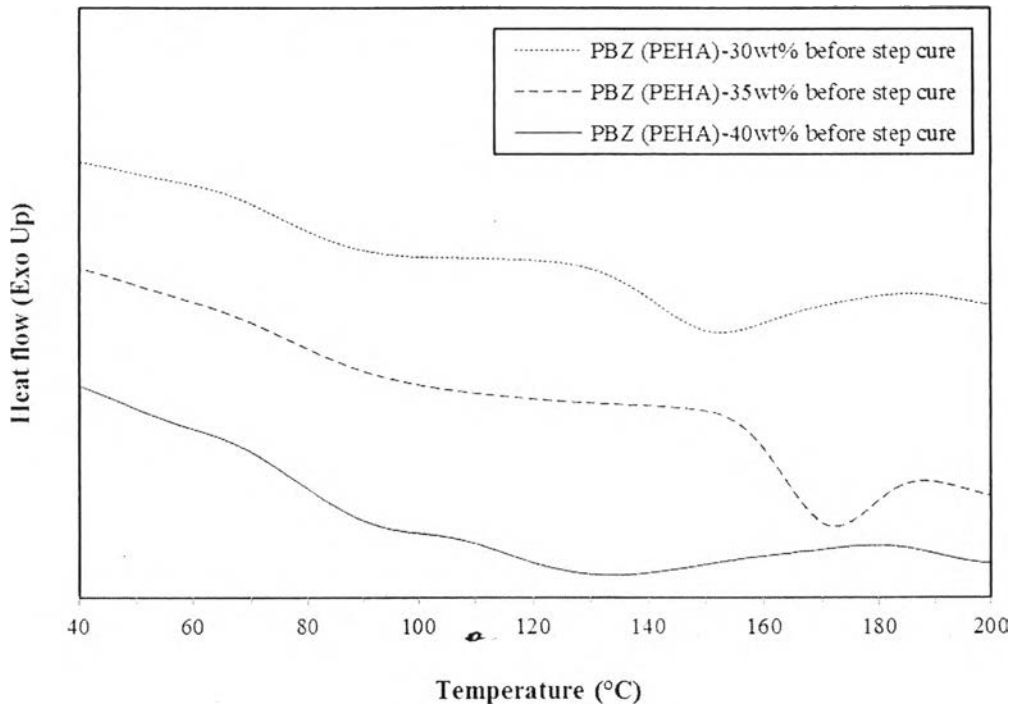

Figure 4.11 DSC thermograms of polybenzoxazine aerogels before curing step with PEHA as reactant.

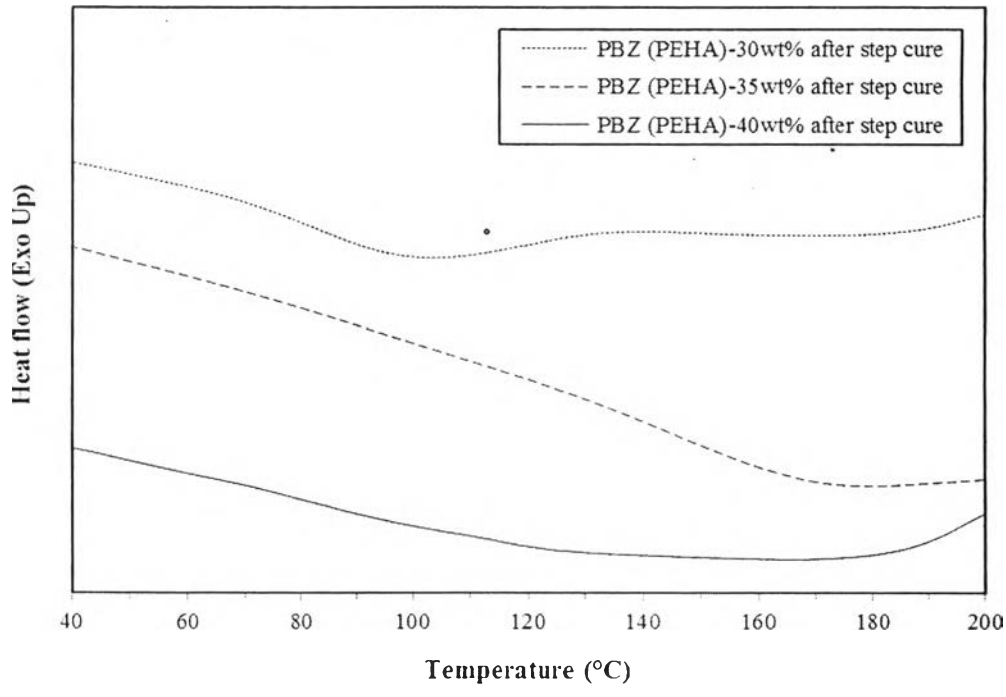

Figure 4.12 DSC thermograms of polybenzoxazine aerogels after curing step with PEHA as reactant.

The TGA thermograms of both polybenzoxazine aerogels were presented in Figures 4.13 and 4.14. The results showed that DETA-derived polybenzoxazine aerogel and PEHA-derived polybenzoxazine aerogel started to lose weight at 200 °C and the highest maximum mass loss rate was observed in the temperature range of 200 - 600 °C, which was caused by the emission of a large amount of volatile materials. The char yield of DETA-derived polybenzoxazine aerogel and PEHA-derived polybenzoxazine aerogel at 800 °C was around 35 and 20 wt%, respectively. The char yield of PEHA-derived polybenzoxazine aerogel was less than the char yield of DETA-derived polybenzoxazine due to a higher molecular weight of PEHA-derived polybenzoxazine. As a result, the carbon-carbon bonds of long aliphatic chains were easily broken at high temperature and, finally, less char yield was obtained (Appendix E). On top of that, the polybenzoxazine-derived from DETA performed a higher thermal stability than polybenzoxazine prepared by Lorjai *et al.* (2009) which was started degradation at 300 °C, with a char yield of 25 wt% at 800 °C.

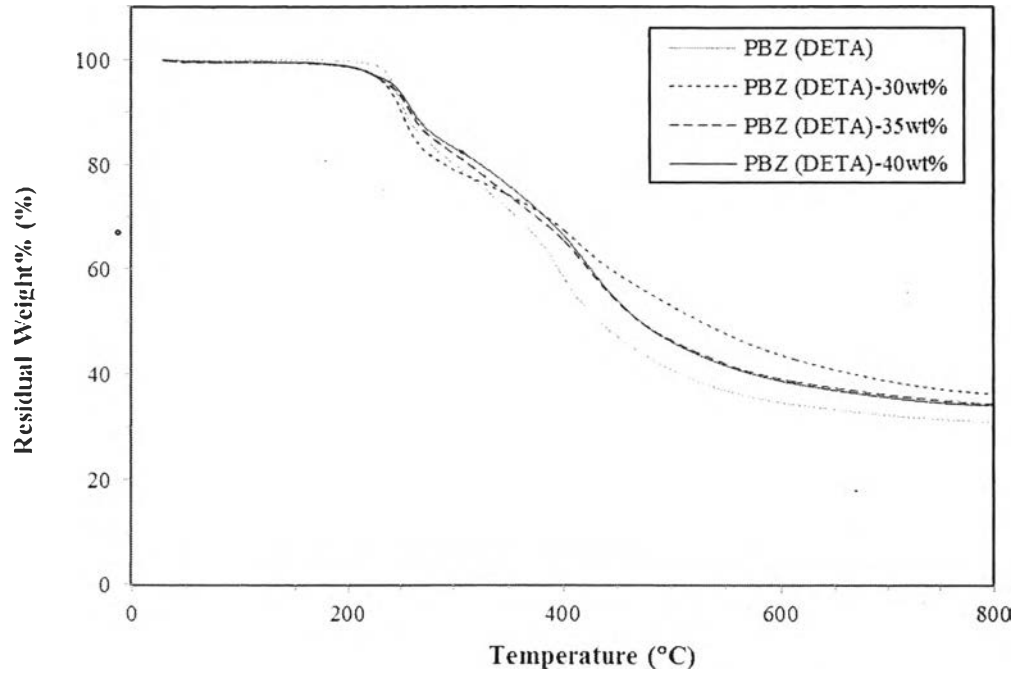

Figure 4.13 TGA thermograms of polybenzoxaine and polybenzoxazine aerogels with DETA as reactant.

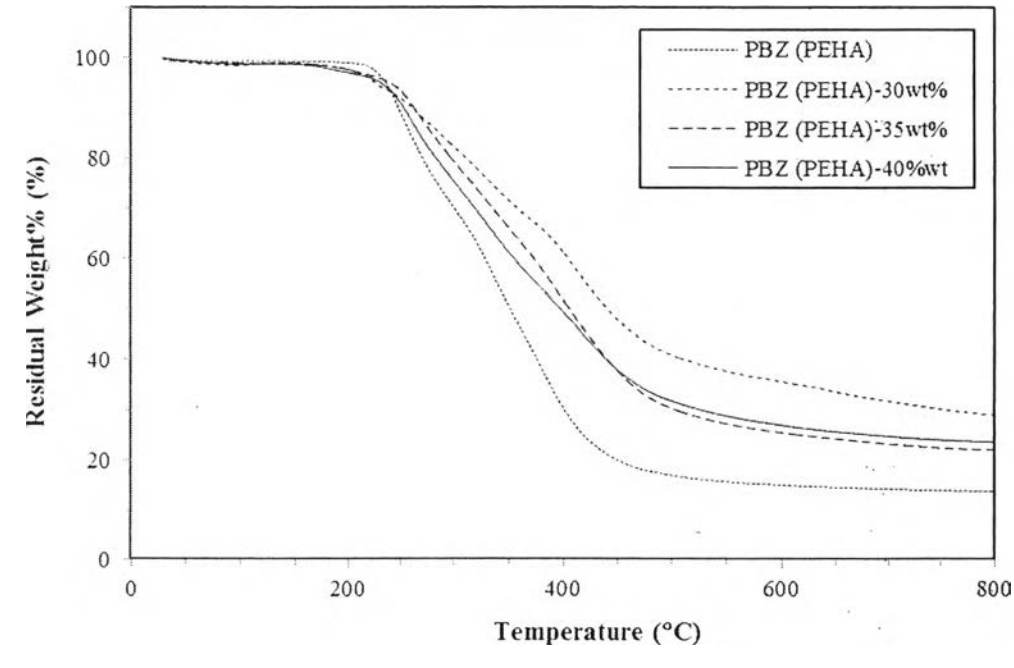

Figure 4.14 TGA thermograms of polybenzoxazine and polybenzoxazine aerogels with PEHA as reactant.

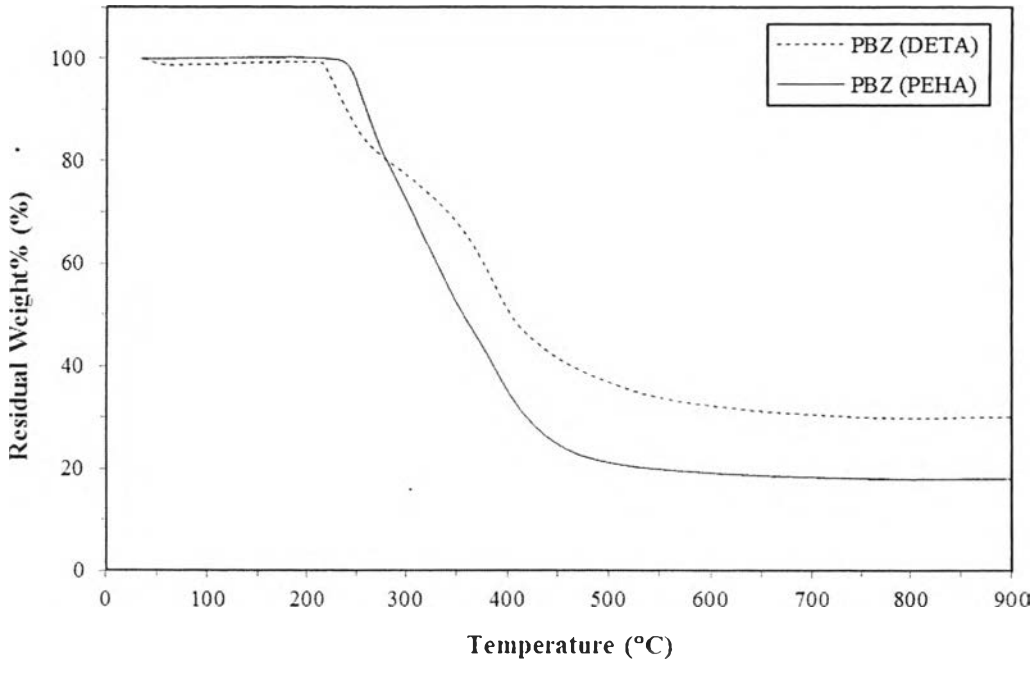

Figure 4.15 TGA thermograms of PBZs derived from DETA and PEHA after heating up to 900 °C (with a heating rate of 20 °C/min).

Figures 4.15, 4.16, and 4.17 illustrate the TGA thermograms of PBZs, pure non-ionic surfactant, and PBZ based organic aerogel with and without PEG-PPG-PEG block copolymer as non-ionic surfactant by two different amine precursors. As for activated carbons derived from PBZ, the char yield at 900 °C of DETA-based activated carbon was 30.14 wt%, while PEHA-based activated carbon was 18.07 wt% at the same temperature. The activated carbon from PEHA-derived PBZ preformed a lower char yield than DETA-based activated carbon at 900 °C due to the carbon-carbon bonds of longer aliphatic chains were easily broken at high temperature. In addition, after burning at 900 °C under N_2 atmosphere, the results showed that the organic aerogels were higher char yield than those organic aerogels loading with non-ionic surfactant because of the losing weight of non-ionic surfactant which did not observe beyond 400 °C (see Figure 4.16).

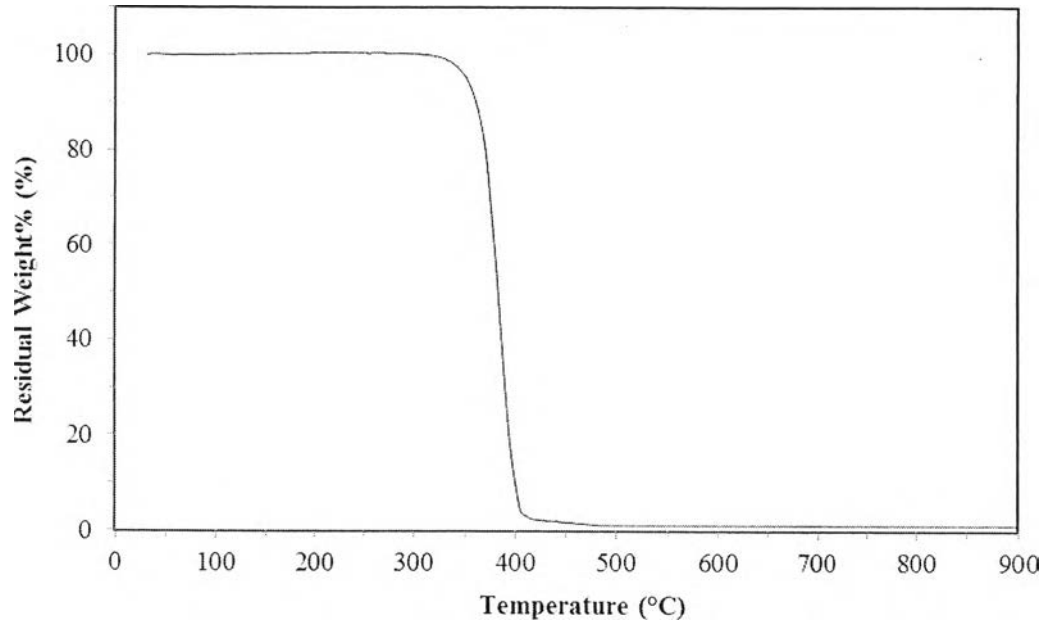

Figure 4.16 TGA thermograms of PEG-PPG-PEG block copolymer after heating up to 900 °C (with heating rate of 20 °C/min).

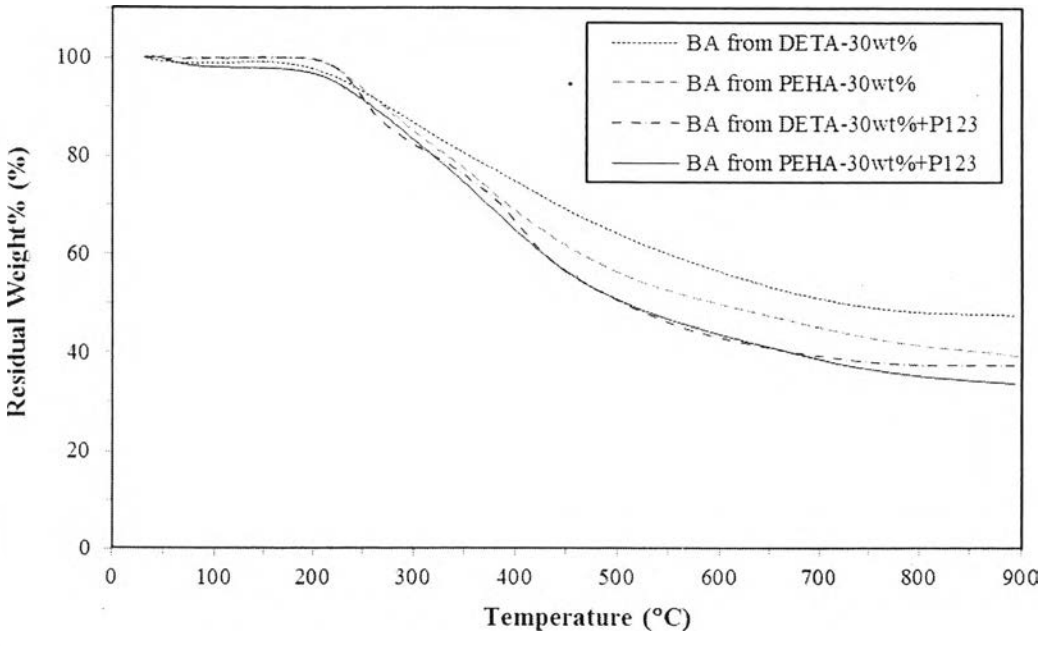

Figure 4.17 TGA thermograms of PBZ aerogels derived from DETA and PEHA with and without non-ionic surfactant (PEG-PPG-PEG block copolymer) after heating up to 900 °C (with heating rate of 20 °C/min).

Table 4.1 The surface property of organic PBZ aerogels derived from DETA and PEHA at different PBZ concentration and their carbon aerogels obtaining at activation temperature of 800 °C

Adsorbents	BET Surface Area (m^2/g)	Micropore Volume (cm^3/g)	Mesopore Volume (cm^3/g)	Total Pore Volume (cm^3/g)	Pore Size (nm)
AC (DETA)	167	0.088	0.071	0.181	1.84
AC (PEHA)	238	0.121	0.155	0.477	0.78
BA from DETA-30w%t	47	0.017	0.029	0.093	2.33
BA from DETA-35wt%	14	0.007	0.070	0.050	1.60
BA from DETA-40wt%	21	0.011	0.063	0.174	2.66
BA from PEHA-30wt%	14	0.007	0.019	0.120	2.17
BA from PEHA-35wt%	52	0.018	-	0.127	2.14
BA from PEHA-40wt%	28	0.013	-	0.052	2.76
CA from DETA-30wt%	312	0.165	0.016	0.258	1.15
CA from DETA-35wt%	368	0.193	0.053	0.288	1.09
CA from DETA-40wt%	376	0.202	0.084	0.344	1.20
CA from PEHA-30wt%	114	0.059	0.015	0.124	1.29
CA from PEHA-35wt%	85	0.045	0.004	0.099	2.48
CA from PEHA-40wt%	44	0.024	0.007	0.155	2.40

*AC = Activated carbon, BA = Organic aerogel, and CA = Carbon aerogel

Table 4.2 The surface property of activated carbon from polybenzoxazine, carbon aerogels, and carbon aerogels containing with non-organic surfactant (P_{123}) at activation temperature of 900 °C

Adsorbents	BET Surface Area (m^2/g)	Micropore Volume (cm^3/g)	Mesopore Volume (cm^3/g)	Total Pore Volume (cm^3/g)	Pore Size (nm)
AC (DETA) at 900 °C	178	0.094	0.047	0.297	1.82
AC (PEHA) at 900 °C	295	0.151	0.238	0.433	0.77
CA from DETA-30wt% (900 °C)	695	0.359	-	0.396	0.65
CA from PEHA-30wt% (900 °C)	304	0.161	0.013	0.179	0.78
CA from DETA-30wt%+P_{123} (900 °C)	665	0.343	0.043	0.386	0.76
CA from PEHA-30wt%+P_{123} (900 °C)	502	0.273	0.007	0.285	0.77

*AC = Activated carbon, CA = Carbon aerogel, and P_{123} = Poly(ethylene glycol)-block-poly(propylene glycol)-block-poly(ethylene glycol)

4.2 Effect of Preparation Method on Polybenzoxazine-based Carbon

Since the bulk polymerization technique prepared by curing polybenzoxazine and following with carbonization and activation processes did not provide good textural property appropriate for adsorption application, a sol-gel technique was proposed to improve the surface properties of the polybenzoxazine-based activated carbon and to compare this surface property with the conventional method due to the satisfied surface property from many works on a sol-gel process (Chaisuwan *et al.*, 2010; Katanyoota *et al.*; 2010, Lorjai *et al.*, 2011).

Table 4.1 shows the BET surface area and other porous characteristics of activated carbons from polybenzoxazine and carbon aerogels, with DETA (diethylenetriamine) and PEHA (pentaethylenehexamine) as amine precursor. In case of DETA as an amine reactant, the result reveals that activated carbon from DETA-derived polybenzoxazine gave the BET surface area of 167 m^2/g and the total pore volume of 0.181 cm^3/g with the micropore volume of 0.088 cm^3/g (by 49 % of total pore volume), whereas the carbon aerogel from DETA-30 wt% of benzoxazine solution showed the BET surface area of 312 m^2/g and the total pore volume of 0.258 cm^3/g with the micropore volume of 0.165 cm^3/g (by 64 % of total pore volume). These results show clearly that the influence of solvent in a sol-gel technique could help generate more porosity in polybenzoxazine structure, especially in producing microporosity of carbon aerogel, as observed from the results of BET surface area and total pore volume for all concentrations of carbon aerogels as compared to the conventional technique (see Table 4.1). Figure 4.18 shows the SEM images of activated carbon from bulk polymerization of DETA-derived PBZ and carbon aerogel from DETA-30 wt% with a magnification of 2,000 times obtained from a JEOL-JSM 8000LV. Activated carbon from DETA-derived polybenzoxazine contained carbon particle with a size range of approximately just under 2 to 3 μm and exhibited a continuous network of carbon particles with open macropores as shown in Figure 4.18a. For carbon aerogel from DETA-30 wt% of benzoxazine solution (Fig. 4.18c), the skeleton of carbon aerogel consisted of an assemble carbon particles in three dimensions with completed interconnected pore structure which was called a sponge-like structure. This observed shape of carbon aerogel was similar with many other works

(Li *et al.*, 2002, Sevilla *et al.*, 2011). In addition, carbon aerogel performed a larger particle size than those particles from activated carbon prepared from bulk polymerization of polybenzoxazine. It was because the effect of solvent during the generation porosity via a sol-gel process had a predominant influence on the particle size of carbon.

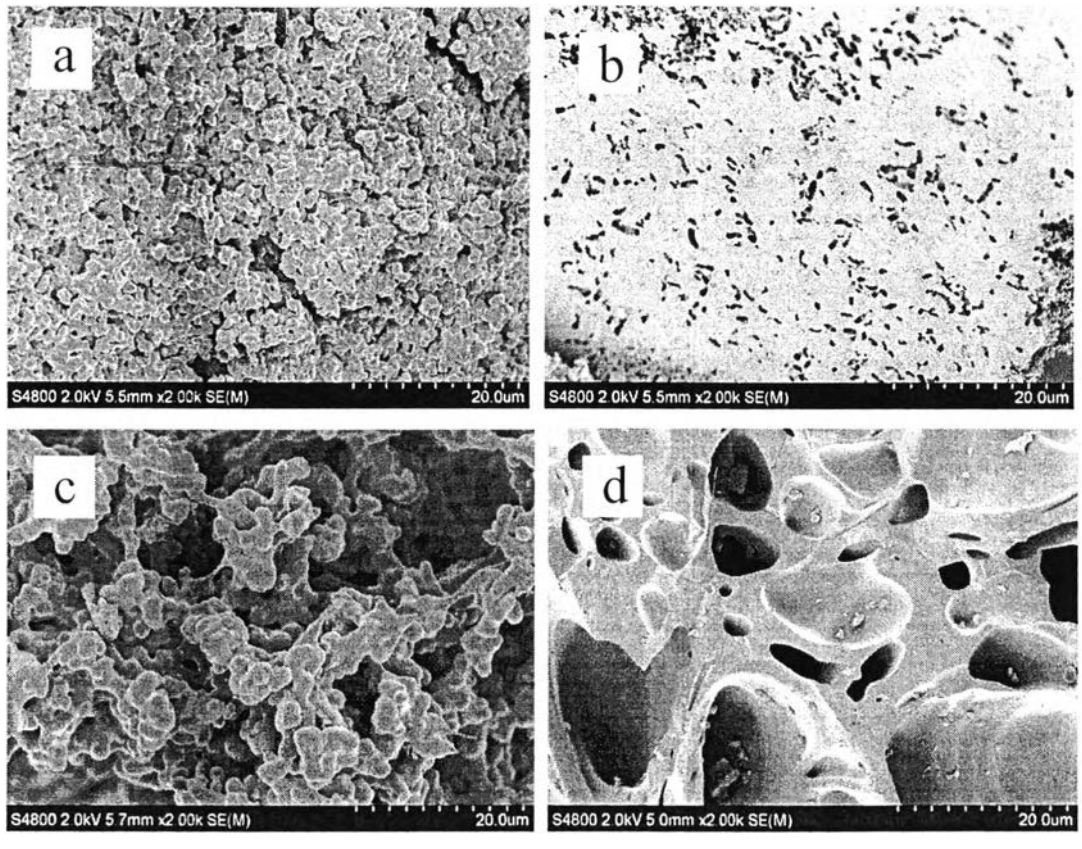

Figure 4.18 SEM images of (a) activated carbon from bulk polymerization of DETA-derived PBZ, (b) activated carbon from PEHA-derived PBZ, (c) carbon aerogel from DETA-30 wt%, and (d) carbon aerogel from PEHA-30 wt%.

Considering PEHA as an amine reactant, the result shows that activated carbon from PEHA-derived polybenzoxazine gave the specific surface area of 238 m^2/g and the total pore volume of 0.477 cm^3/g with the micropore volume of 0.121 cm^3/g (by 25 % of total pore volume), while carbon aerogel from PEHA-30 wt% of benzoxazine monomer provided the BET surface area of 114 m^2/g and the total pore

volume of 0.124 cm^3/g with the micropore volume of 0.059 cm^3/g (by 48 % of total pore volume). This carbon aerogel showed a lower BET surface area and a lower total pore volume compared to those results from the bulk polymerization technique. It was because the small pores within aerogel structure were fused with some residual solvents during carbonization and activation processes as a result of pore collapse; therefore, the non-uniform porosity in the solid network was observed in Figure 4.18 (d). However, carbon aerogel exhibited higher percentage of micropore volume to total pore volume than activated carbon from bulk polymerization of PEHA-derived PBZ owing to the effect of solvent on the porous material preparation. Another effect from different amine precursors will be further discussed.

4.3 Effect of Benzoxazine Monomer Concentrations on Polybenzoxazine-based Organic Aerogels and Carbon Aerogels

Since a sol-gel technique provided good textural property of carbon aerogel as mentioned above, it is of interest to find out the suitable porous carbon for carbon dioxide adsorption application. The benzoxazine content was varied to observe the surface property of the PBZ-based organic aerogels and carbon aerogels. For PBZ-based organic aerogels, three concentrations of benzoxazine monomer were varied: 20, 25, and 30 wt%.

Figure 4.19 shows the SEM images of fully cured DETA-derived PBZ organic aerogels at the monomer concentrations of 20, 25, and 30 wt% with a magnification of 2500 times received from a TM3000/Hitachi. As for the DETA-based organic aerogels with monomer concentrations of 20 and 25 wt%, both monomer concentrations showed an agglomeration of spherical particles with diameters of 2 to 4 μm; likewise, they performed an interconnected structure in three dimensions with large open macropores between 20 and more than 30 μm. However, DETA-based organic aerogel from 20 and 25 wt% of benzoxazine solutions was not suitable for the application of carbon dioxide capture because their pore size were too large and could be observed by the naked eyes as shown in Figures 4.19 (a) and (b). In case of DETA-based organic aerogel with 30 wt%, it exhibited a smaller size of particles at approximately less than 2 μm as compared to those lower concentrations. Additional-

ly, it had small macropores (less than 10 μm) with interconnected macroporosity in three dimensions as observed in Figure 4.19 (c).

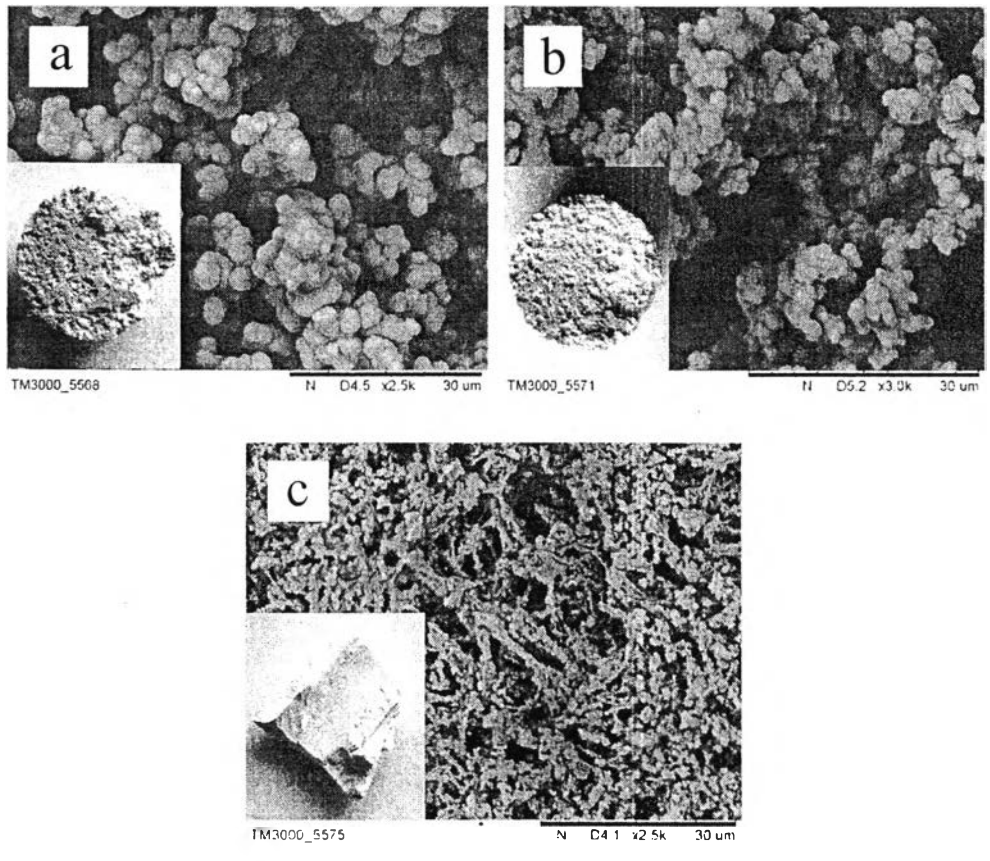

Figure 4.19 SEM images of (a) fully cured DETA-derived PBZ aerogel at 20 wt%, (b) 25 wt%, and (c) 30 wt% of monomer solutions.

For DETA-derived PBZ, benzoxazine content was varied at 30, 35, and 40 wt% to observe the textural properties.

After the curing step, the complete porous structure of organic aerogel was obtained. Table 4.1 shows the textural properties of PBZ-based organic aerogels from DETA and PEHA as amine precursor. For DETA-derived PBZ organic aerogels with 30, 35, and 40 wt% of benzoxazine solutions, they provided the BET surface of 47, 14, and 21 m^2/g, the total pore volume of 0.093, 0.050, and 0.174 cm^3/g, and the pore diameter of 2.33, 1.60, and 2.66 nm, respectively, which were performed in the mesopore size. In case of PEHA-derived PBZ organic aerogels, at 30,

35, and 40 wt% of benzoxazine solutions showed the specific surface area of 14, 52, and 28 m^2/g, the specific pore volume of 0.120, 0.127, and 0.052 cm^3/g, and the pore size of 2.17, 2.14, and 2.76 nm, respectively. Nevertheless, these surface properties, such as specific surface area, specific pore volume, and pore diameter did not change significantly with increasing the amount of benzoxazine content for both amine precursors.

After carbonization under nitrogen atmosphere and activation with CO_2 at 800 °C for 2 hours, organic aerogel was transformed to carbon form called carbon aerogel. In comparison, carbon aerogel exhibited the obvious change on textural properties over organic aerogel because carbonization and activation processes led to the generation of new pores or voids in the structure of aerogel as observed in Table 4.1. These results strongly agree with many studies (Li *et al.*, 2002; Al-Muhtaseb and Ritter, 2003). As for DETA-based carbon aerogels with 30, 35, and 40 wt% of benzoxazine solution, they exhibited the BET surface area of 312, 368, and 376 m^2/g, the total pore volume of 0.258, 0.288, and 0.344 cm^3/g, and the pore size of 1.15, 1.09, and 1.20 nm, respectively, which was in the range of micropore. Although varying the benzoxazine content did not have a dramatic impact on the resulting textural properties of carbon aerogels (Table 4.1), it seemed to provide the distinctive results on the SEM images. Figure 4.20 shows the SEM images of carbon aerogel from DETA kept at monomer concentration of 30, 35, and 40 wt% with a magnification of 600 and 2000 times obtained from JEOL-JSM 8000LV. Figure 4.20 (a) and (b) shows that these spherical particles on carbon aerogel with 30 wt% of monomer solution were shaped like "the pearl necklace" as the similar feature appeared in the study of Cotet *et al.* (2007). Additionally, these particles not only had a spherical shape, but they could also generate the interconnected macropores within the carbon skeleton. In contrast, at 35 or 40 wt% of monomer solution, some macropores or no macropores could be observed on the carbon aerogel due to the damaging of small pores during the thermal treatments (Fig. 4.20c - f). In detailed, these features might be often found at high benzoxazine concentration because the generation of small pores would led to the trap of some remaining solvent within aerogel structure. After that, these pores were completely destroyed during heating via curing step or carbonization.

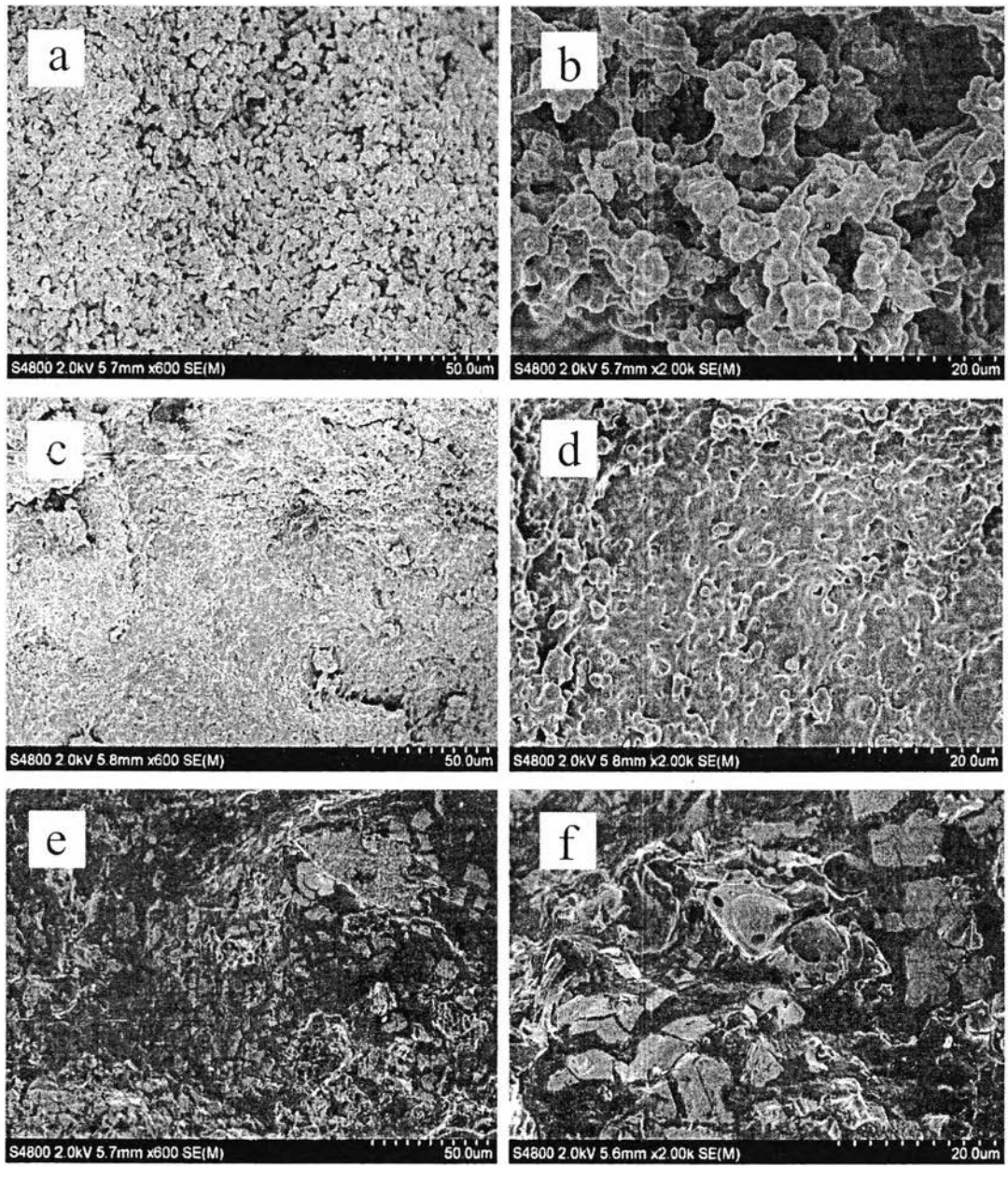

Figure 4.20 SEM images of DETA-derived PBZ carbon aerogel at (a) 30 wt%, (b) 30 wt%, (c) 35 wt%, (d) 35 wt%, (e) 40 wt%, and (f) 40 wt% of monomer solutions; low magnification for (a), (c), and (e); high magnification for (b), (d), and (f).

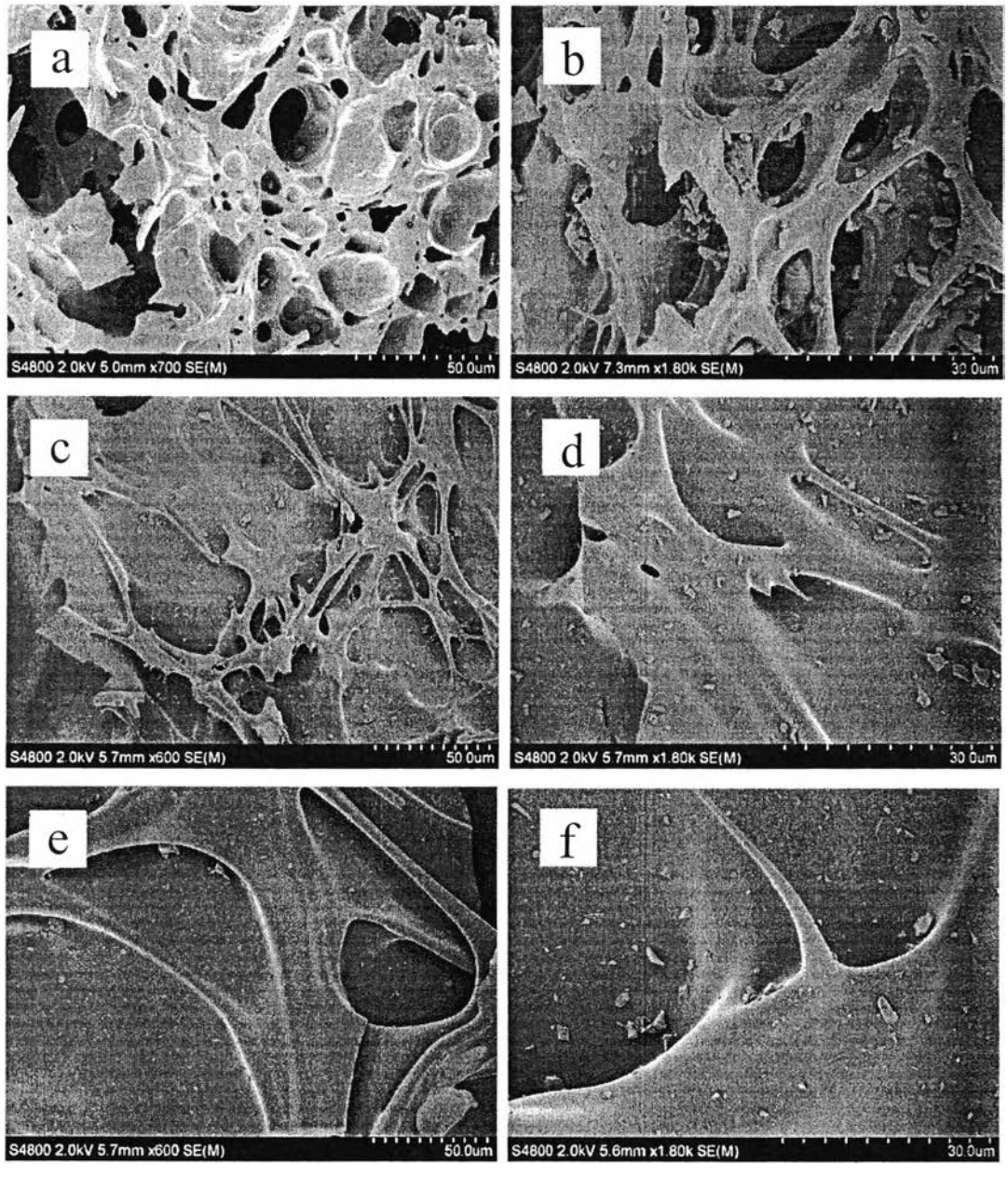

Figure 4.21 SEM images of PEHA-derived PBZ carbon aerogel at (a) 30 wt%, (b) 30 wt%, (c) 35 wt%, (d) 35 wt%, (e) 40 wt%, and (f) 40 wt% of monomer solutions; low magnification for (a), (c), and (e); high magnification for (b), (d), and (f).

Turning to consider about carbon aerogels from PEHA as reactant, carbon aerogels prepared from 30, 35, and 40 wt% of benzoxazine solutions performed the specific surface area of 114, 85, and 44 m^2/g, the specific pore volume of 0.124, 0.099, and 0.155 cm^3/g, and the pore diameter of 1.29, 2.48, and 2.40 nm, respective-

ly (see Table 4.1). In this case, the trends of BET surface area and the micropore volume slightly decreased with increasing the amount of benzoxazine content due to the difficultly of removing volatile matters from carbon aerogel during carbonization and activation processes.

Furthermore, the SEM images of those carbon aerogels from different monomer concentrations were shown in Figure 4.21. These results reveal that, at high monomer content of 40 wt%, all of the open macropores disappeared from the surface of the carbon aerogel as a result of decreasing specific surface area as shown in Figure 4.21 (e) and (f). Whereas, non-uniform macropores with pore size larger than 30 μm were observed at low benzoxazine content of 30 wt% as shown in Figure 4.21 (a) and (b).

4.4 Effect of Chain Lengths of Amine Precursors on Activated Carbons from Polybenzoxazine and Polybenzoxazine-based Carbon Aerogels

One of the most factors that affected directly on the microstructure was the type of amine as mentioned in the work of Thubsuang *et al.* (2014). In this study, the two different types of polybenzoxazines were synthesized from phenol, formaldehyde and two different amine precursors that were diethylenetriamine (DETA) and pentaethylenehexamine (PEHA).

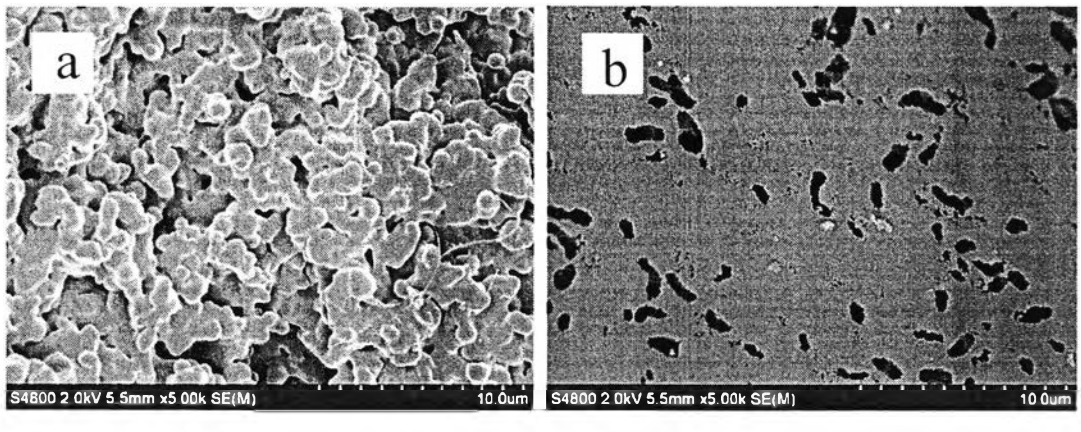

Figure 4.22 SEM images of activated carbon from bulk polymerization of (a) DETA-derived PBZ and (b) PEHA-derived PBZ, with a magnification of 5,000 times.

Table 4.1 demonstrates the textural properties of PBZs from two different amine precursors. The results revealed that activated carbon from bulk polymerization of DETA-derived PBZ showed the BET surface area of 167 m^2/g, the total pore volume of 0.181 cm^3/g, and the pore size of 1.84 nm, whereas the activated carbon from PEHA-derived PBZ displayed the specific surface area of 238 m^2/g, the specific pore volume of 0.477 cm^3/g, and the pore size of 0.78 nm. It can be observed that PEHA-based activated carbon had a higher surface area and a larger total pore volume than DETA-derived PBZ activated carbon due to the more generation of micropore volume on the surface of PEHA-derived activated carbon as observed in Table 4.1. In detail, the smaller pore size of PEHA derived PBZ was found. The main reason might occur from higher hydrogen bonding between long aliphatic chains of amine in PEHA-derived PBZ, resulting in a dense packing structure of the polymer and, consequently, smaller pores were created. A similar trend was observed with the activation temperature of 900 °C as shown in Table 4.2.

As summarized in Table 4.1, carbon aerogels derived from DETA and PEHA composed of both micropores and mesopores, where the pore size was in the micropore range. However, DETA-based carbon aerogels contained more of micropores and provided higher surface area than PEHA-based carbon aerogels. It was because the preparation of DETA-derived PBZ on carbon aerogel was successful which was confirmed by the results from SEM images as shown in Figure 4.20. These SEM images were similar to the other studies on carbon aerogel preparation (Lorjai *et al.*, 2009; Kwon *et al.*, 2014). In conversely, carbon aerogels from PEHA-derived PBZ illustrated the collapsed pores on their surfaces as evidenced from the SEM images in Figure 4.21, resulting in the low surface area and micropore volume as tabulated in Table 4.1.

4.5 Effect of Activation Temperatures on Activated Carbon from Polybenzoxazine and Polybenzoxazine-based Carbon Aerogel

Since the creation of high surface area and pore volume in the porous materials has become necessary in various applications, e.g., catalysis, membrane, and

adsorption (Smirnova *et al.*, 2009; Hsu *et al.*, 2013; He *et al.*, 2014). Consequently, varying activation temperature was the best way to find out the suitable condition for improvement of the textural properties on the porous structures applying in carbon dioxide capture. In the present study, those materials from PBZ were activated under CO_2 atmosphere for 2 hours at two different activation temperatures of 800 and 900 °C.

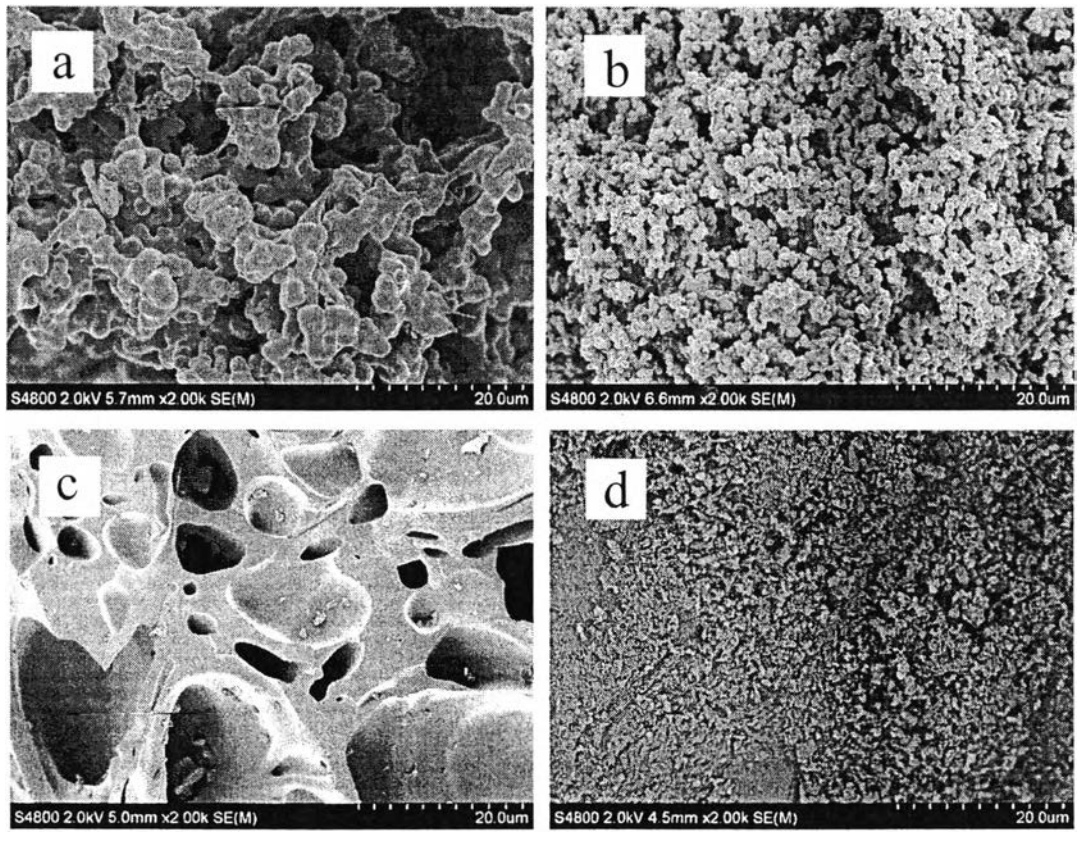

Figure 4.23 SEM images of (a) carbon aerogel from DETA-30 wt% at activation temperature of 800 °C, (b) carbon aerogel from DETA-30 wt% at activation temperature of 900 °C, (c) carbon aerogel from PEHA-30 wt% at activation temperature of 800 °C, and (d) carbon aerogel from PEHA-30 wt% at activation temperature of 900 °C.

The textural properties of the PBZ-based activated carbons after activation at 800 ° and 900 °C are summarized in Table 4.1 and 4.2, respectively. Comparing

between two DETA-derived PBZ activated carbons at activation temperature of 800 ° and 900 °C, they had a surface area of 167 m^2/g and 178 m^2/g and pore volume of 0.181 and 0.297 cm^3/g, respectively. There was a slight rise in surface area and pore volume at higher activation temperature; likewise, a similar trend was observe in the PEHA-based activated carbons at different activation temperatures as shown in Tables 4.1 and 4.2.

Tables 4.1 and 4.2 show the BET surface area and other pore characteristics of carbon aerogel samples at two different activation temperatures. In case of carbon aerogel from DETA with 30 wt%, at activation temperature of 900 °C, it indicated the surface area of 695 m^2/g, pore volume of 0.396 cm^3/g, and pore size of 0.65 nm. Interestingly, the activation temperature of 900 °C could give activated carbon with double the surface area and pore volume, especially for micropore volume, as compared to 30 wt% of DETA-based carbon aerogel at activation temperature of 800 °C. It is obvious that the higher surface area and pore volume is dependent on the activation temperature like those proposed by Robertson and Mokaya (2013). Figure 4.23 exhibits the SEM images of 30 wt% of DETA-derived PBZ carbon aerogels at different activation temperature of 800 and 900 °C. At higher activation temperature, the carbon particles (less than 1 μm) are smaller than those obtained from the activation condition at 800 °C with interconnected macropores in three dimensions as observed in Figure 4.23 (b). In the similar case, a larger increase in surface area (or pore volume) from 114 m^2/g (0.124 cm^3/g) to 304 m^2/g (0.179 cm^3/g) was observed for 30% of PEHA-based carbon aerogel activated at 900 °C (see Tables 4.1 and 4.2), with smaller carbon particles on the surface of carbon aerogel as observed in Figure 4.23 (d).

4.6 Effect of Non-ionic Surfactant (PEG-PPG-PEG Block Copolymer) on Polybenzoxazine-based Carbon Aerogel

According to the collapse of pores in the preparation of carbon aerogel materials, especially appeared in all carbon aerogels from PEHA as an amine reactant (Table 4.1 and Figure 4.21), another technique was employed to improve the surface properties of these carbon aerogels. Since, non-ionic surfactant played a good role to

disperse the aggregated molecule of PBZ during the preparation of aerogel as mentioned in the work of Thubsuang (2015), in this work, PEG-PPG-PEG block copolymer was used as a non-ionic surfactant (by 6 wt% of benzoxazine content).

All PBZ-based carbon aerogels with and without non-ionic surfactant are summarized in Table 4.2. For 30 wt% of DETA-based carbon aerogel, adding surfactant did not help generate more porosity within its structure. As a result, the similar textural properties were observed, with a surface area of 665 m^2/g, pore volume of 0.386 cm^3/g and a micropore volume of 0.343 (by 89 % of total pore volume). Conversely, the textural properties of the 30 wt% PEHA-derived PBZ carbon aerogel were a significantly improve. The surface area was rise from 304 m^2/g to 502 m^2/g (with surfactant) and pore volume from 0.179 cm^3/g to 0.285 cm^3/g (with surfactant). With the aid of non-ionic surfactant, the porous structure of carbon aerogel was less packed and this result agreed well with the study of Wang *et al.* (2011). This confirmed that the non-ionic surfactant successfully helped disperse the aggregated molecules of PEHA-derived PBZ.